Radiation damage and uranium concentration in zircon as assessed by Raman spectroscopy and neutron irradiation

A.E. Marsellos[1,2,*] and J.I. Garver[2]

[1]Department of Earth and Atmospheric Sciences, State University of New York, Albany, New York 12222, U.S.A.
[2]Department of Geology, Union College, Schenectady, New York 12308, U.S.A.

Abstract

Radiation damage of natural and synthetic zircon grains is evaluated by Raman spectroscopy to understand annealing and stability of fission tracks. Analyses focus on a suite of 338 Paleozoic detrital zircon grains from metamorphosed strata in the Hellenic forearc that were variably annealed by a Miocene thermal event, as well as a suite of 97 synthetic zircon grains. The Raman wavenumber shift of v_3 [SiO$_4$] reveals that radiation damage and damage distribution in this suite mainly depends on uranium concentration. In zircon with similar uranium concentration, the Raman wavenumber shift allows for the determination of radiation damage in different crystals, which is a function of effective accumulation time. Nine detrital zircons grains with moderate radiation damage were stepwise annealed at 1000 and 1400 °C, which resulted in progressive removal of radiation damage revealed in an increase of v_3 [SiO$_4$] peak positions. For a partly reset sample that was brought to temperatures of ~350 °C in a geologic setting (Hellenic forearc), we use the Raman measurements and uranium determination to estimate a Zircon Damage Discrimination Factor (Z_{RDD}), which is our attempt to estimate only radiation damage in single grains by accounting for affects of the uranium atom in the Raman wavenumber. This discrimination allows for a separation of zircon fission track (ZFT) ages of single ages based on grains that have a low track retention (high damage, fully reset grain), thus refining the age determination of cooling in a rock that shows variable resetting.

Keywords: Geochronology, zircon fission track, radiation damage, uranium content, Raman spectroscopy

Introduction

Radiation damage in zircon is manifested by a decrease in crystallinity, the production of color, a decrease in density, an increase in water, and volume expansion (Ewing et al. 2003 and references therein). Because zircon is so widely used in geochronology, understanding the relationship of crystallinity to radiation damage is very important, and in the case of fission track dating, crystallinity or lack of crystallinity is inferred to be the primary factor that affects track retention and annealing (Kasuya and Naeser 1988). Therefore, radiation damage in zircon is central to understanding the kinetics of track formation and stability, the bounds of closure temperature, and the environmental conditions of track fading or annealing at elevated temperatures.

For this work, we are primarily interested in how radiation damage affects the material properties of zircon that we routinely analyze using fission-track dating (Garver 2008). There are two primary effects that are of concern. One is that radiation damage increases the chemical reactivity of a zircon, and this affect facilitates etching and track revelation in the lab: fission tracks in damaged grains etch easily and quickly. The other is that radiation damage changes the annealing and closure temperature in zircon. Damaged grains are easily annealed when brought to elevated temperatures (~200 °C and greater), and damaged grains appear to have a lower closure temperature compared to grains

with little or no damage (see Garver et al. 2005 and references therein). As such, we measured radiation damage and crystallinity in a zircon using Raman spectroscopy to aid our understanding of fission tracks in zircon.

Trace concentrations of U^{4+} and/or Th^{4+} substitute for Zr^{4+} in natural zircons (ZrSiO$_4$), and the radioactive decay of U and Th causes internal radiation damage in the crystal that increases with accumulation time (e.g., Holland and Gottfried 1955; Ahrens 1965; Ahrens et al. 1967). Due to similarities in the ionic radius of U^{4+} and Th^{4+} (1.00–1.05 Å) (Shannon 1976), these elements replace Zr^{4+} and occur in zircon with abundances typically ranging from tens to thousands of parts per million (Speer 1980). The emission of an α-particle during decay causes the displacement of several hundred atoms, and the recoil of the radiogenic atom (uranium and its prompt daughter isotopes) produces several thousand atomic displacements within the lattice (e.g., Weber et al. 1994; Farnan and Salje 2001; Fleischer 2003). Zircon grains with higher U and Th (e.g., 1000 ppm) contain more radiation damage than those with lower uranium (e.g., 200 ppm) given a comparable effective accumulation time of radiation damage (i.e., similar thermal history). Although this observation seems intuitively obvious, the difference in radiation damage from crystal to crystal in the same rock can have profound implications for the geochronologic systematics of that sample (i.e., see discussion in Bernet and Garver 2005).

When a zircon grain is analyzed in the laboratory, one would like to know the total amount of accumulated radiation damage

* E-mail: marsellos@gmail.com

in that crystal. Total radiation damage or the crystallinity of zircon is a function of: (1) the presence of actinides (effectively only uranium and thorium); (2) the time or duration of radioactive disintegration; and (3) removal of damage or annealing at elevated temperatures. The duration of disintegration (which produces damage), and annealing (which removes damage) can be complicated because annealing and partial annealing are poorly understood. Whereas radioactive decay is continuous, the annealing of the resulting damage is not, and it occurs at different rates above ~150–200 °C. Therefore, the time-temperature history (or thermal history) is an important aspect of total radiation damage in a particular crystal, and, unfortunately, this is almost always incompletely known. For the sake of discussion, the two opposite effects are integrated and referred to as the "effective accumulation time," which is defined as the time required to produce the total radiation damage present in a crystal.

In this paper, we investigate the influence of uranium content on radiation damage in single natural, synthetic, and in annealed natural zircon grains. The amount of disorder caused by radiation damage to the zircon lattice can be evaluated by Raman spectroscopy by measuring changes in the frequency and width (full-width half maximum, FWHM) of the SiO_4 vibrations (e.g., Nasdala et al. 1995, 1998, 2001, 2003; Wopenka et al. 1996; Zhang et al. 2000a, 2000b; Balan et al. 2001; Geisler et al. 2001, 2003a, 2003b, 2005; Hogdahl et al. 2001; Geisler 2002; Palenik et al. 2003). Changes of the Raman vibrational frequency also have been investigated using hafnium-doped synthetic zircon grains, containing no uranium. Raman spectroscopic measurements of synthetic and annealed natural radiation-damaged zircon grains are used to define the range of Raman wavenumber frequency corresponding to different degrees of radiation damage. A primary goal of this research is to better understand the effect of radiation damage on the stability of fission tracks in zircon.

COMPOSITION OF ZIRCON AND RADIATION DAMAGE

Many minerals have a zircon structure (e.g., xenotime, thorite, and coffinite), but only hafnon ($HfSiO_4$) and zircon ($ZrSiO_4$) are identical except for small differences in bond lengths and angles (Speer and Cooper 1982). The ionic radius of Hf^{4+} (0.83 Å) is only slightly smaller than that of Zr^{4+} (0.84 Å), and the unit-cell dimensions of hafnon are correspondingly similar to those of zircon. A compilation of published Hf^{4+} values in natural zircon reveals a mean value of 1.71 wt% HfO_2, with a range from ~0.6–7.0 wt% (Ahrens and Erlank 1969). Typical concentrations of uranium and thorium in natural zircon grains fall between 5–4000 ppm for uranium and 2–2000 ppm for thorium (Speer 1980). Typical natural detrital zircon grains have a mean uranium concentration of ~419 ppm, a mode of ~140 ppm, and an average Th/U ratio of 0.5 (Garver and Kamp 2002).

Radiation damage in zircon accumulates in the crystal structure over time through the radioactive decay of actinides. This damage is crystalline disorder caused by the atomic interaction of decay products, and it results in several changes in the crystal properties. With increasing radiation damage, these changes include a decrease in density, increase in volume, increase in internal disorder, and other important effects such as the accumulation of color centers in the red series (see Garver and Kamp 2002). Of particular significance are the actinides,

principally U and Th, which decay through time, and thus are the basis of radiometric dating of the host crystal. The decay of these actinides results in radiation damage in the crystal, and because healing (or annealing) is relatively slow, the damage tends to accumulate with time provided that the crystal is held at relatively low temperatures (<200 °C). Radiation damage is a general term for several direct and indirect effects produced by both α-particles and fission fragments. Considering the relative elemental abundances, relative decay rates, and the energy released per decay, zircon grains are mainly affected by α-recoil damage caused by the decay of the ^{238}U isotope (see Wagner and Van Den Haute 1992). α-damage is driven by the ejection of a helium atom and the recoil of the parent atom: the former is the basis of the rapidly evolving helium dating, and the latter is what causes most of the internal damage to the crystalline structure of a zircon (see Reiners 2005 and Nasdala et al. 2004, respectively). Note that in the decay of a single atom of ^{238}U to ^{206}Pb, eight helium atoms are ejected and eight separate recoil events occur in the decay chain (see Ellsworth et al. 1994).

A key point is that over time, these recoil events cause considerable damage to the crystal, and that damage changes the material properties of the zircon. A typical zircon that spends hundreds of millions of years in near-surface conditions, such as in a shallow-buried sedimentary basin, accumulates this progressive radiation damage (Garver and Kamp 2002). Most zircon grains with typical uranium concentrations (100–500 ppm) receive enough damage over tens to hundreds of millions years to become partly disordered, or transitional between crystalline and metamict end-members. A metamict zircon is characterized by total disorder, and is generally defined a crystal that is amorphous (easily measured using X-ray scattering; Ellsworth et al. 1994). To reach this state of damage, a crystal must receive a critical amorphization dose of radiation damage (Holland and Gottfried 1955; Ewing 1994). There are several ways that this amorphization dose can be expressed, but the most widely used is the number of α-events per mg of crystal. It is commonly assumed that a metamict zircon has received an internal radiation dose of ~2.0 to 8.0×10^{15} α-events/ mg (Chakoumakos et al. 1987; Woodhead et al. 1991; Ellsworth et al. 1994; Weber et al. 1994). In other words, zircon can progress through a continuum from being fully crystalline (no damage), transitional (moderate damage), to metamict (full damage) (see Garver and Kamp 2002). Most fission track (FT)-dated zircons are transitional in this qualitative scale, and there is a wide range of internal damage that we should expect in typical zircon suites. Thus, materials properties commonly vary from grain to grain, to a significant degree.

There appears to be a clear relationship between radiation damage in zircon and Raman frequencies. A shift to higher-frequency Raman wavenumbers and smaller FWHM of the asymmetrical Si-O stretching bond due to structural recovery of partially metamict zircons (Geisler et al. 2002) has been observed after low-temperature hydrothermal conditions. The Si concentration appears also to be inversely correlated with the U concentration, which is remarkable because U is expected to substitute Zr^{4+} as U^{4+} only (Geisler et al. 2005). Heat treatment of a radiation-damaged zircon may cause marked frequency increase and only moderate FWHM decrease (Nasdala et al. 2003). Thus, structural reconstitution of the zircon by these annealing processes

may not cause the reestablishment of each original bond (Geisler et al. 2001; Nasdala et al. 2002 and references therein).

EXPERIMENTAL METHODS

A total of 34 samples of detrital zircon from the Hellenic fore-arc ridge (Greece) were irradiated with thermal neutrons to induce fission in ^{235}U and subsequently fission track ages were determined on individual grains (Marsellos et al. 2010). During this analytical procedure, the uranium concentration of 338 detrital zircon grains was determined for specific areas of prepared zircon grains (Wagner and Van Den Haute 1992). For the FT analysis (and uranium determination), zircon grains were mounted in Teflon, cut with silicon carbide abrasive, and polished (9 and 1 μm diamond slurry). Only zircon grains cut parallel to the c-axis were chosen for FT dating and subsequent Raman analysis.

Zircon grains do not always have a homogeneous distribution of uranium, and they may have complex zoning. An important aspect of our analysis is that because we have done neutron irradiation with an external detector, we have a map of the uranium distribution for each single zircon grain. For Raman spectroscopy, we analyzed the same area of the zircon that was analyzed during FT analysis. This approach means that we analyzed grains with relatively uniform uranium distribution because in FT analysis we tend to avoid grains with complex uranium zonation, inclusions, and other irregularities. Therefore, when we investigated the relationship between the broadening of FWHM, the wavenumbers of v_1 [SiO$_4$] and v_3 [SiO$_4$] (Fig. 1), and the intensity ratio of v_1 [SiO$_4$] and v_3 [SiO$_4$], we are assured that we have selected zircons with the least internal complexity.

Raman measurements were conducted with a high-resolution Jobin Yvon LabRam 300 Raman using a solid-state laser at 632.817 nm with 20 mW of laser power. The scattered Raman light was collected in 180° backscattering geometry and dispersed by a grating of 1800 grooves/mm. The slit width was 100 μm and the spectral resolution ~2.2 cm^{-1}. A 100× objective and a confocal hole of 400 μm were used for all measurements, yielding an axial (depth) resolution of 2 μm or less [using the "separation between spectra" criterion by Tabaksblat et al. (1992)], and the beam diameter was ~2 μm.

For the annealing experiment, nine natural zircon grains with uranium concentration ranging from 10–1000 ppm were analyzed by Raman spectroscopy before and after stepwise heating at one atmosphere in air at 1000 and 1400 °C in pyrophyllite capsules. Before and after the first annealing (at 1000 °C for 96 h), an average was calculated for the Raman parameters from three separate spectral acquisitions. After the second annealing (1400 °C for 24 h), an average was calculated from five Raman measurements. Zircon grains were photographed before and after annealing using a digital camera to map the areas measured by Raman. Finally, a suite of 57 synthetic zircon grains containing no uranium (and therefore no radiation damage) were examined once using Raman spectroscopy, and these grains provide a reference for zero radiation damage in a zircon.
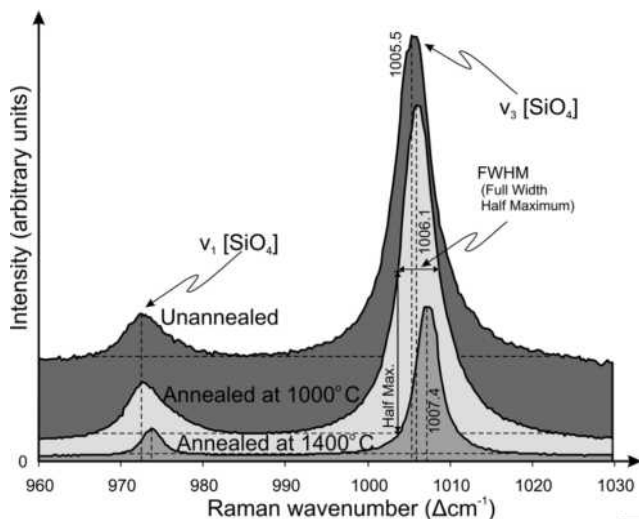

FIGURE 1. Raman spectra from a single zircon from a quartzite from Peloponnese (Greece) measured before and after two successive annealing steps (1000 and 1400 °C).

RESULTS AND DISCUSSION

Annealing experiments

It is necessary to define a high-damage end-member zircon from the literature, before the results from the present work can be discussed. Nearly metamict zircon grains with 1300–3100 ppm uranium show a very low frequency of ~995 Δcm^{-1} in the v_3 [SiO$_4$] band (Nasdala et al. 2004). For example, a very high-uranium zircon with 5600 ppm uranium from Sri Lanka shows a v_3 [SiO$_4$] frequency of 1007.7 Δcm^{-1} after annealing, and before annealing it had an undetectable v_3 [SiO$_4$] frequency (i.e., well below 995 Δcm^{-1}). Thus, this particular grain shows a "Raman annealing range" of at least 12 cm^{-1}, and the full extent of the possible range of radiation damage is estimated from the two boundaries defined by the metamict and the annealed condition of this specific high-uranium zircon from Sri Lanka (Fig. 2). In contrast, low- to medium-uranium zircon grains in this study show a much narrower range of wavenumbers of the v_3 [SiO$_4$] values than high-uranium zircons.

Our annealing experiment shows that full annealing (1400 °C for 24 h) returns the measured frequency of v_3 and v_1 [SiO$_4$] to Raman wavenumber values of undamaged crystalline zircon. Naturally the medium- and high-uranium zircon grains have a larger change in the absolute Raman wavenumber of the v_3 [SiO$_4$] frequency (Fig. 2), because they had more internal damage. Regardless of the total amount of radiation damage, low-uranium zircon grains with less than ~200 ppm show only small changes in Raman wavenumber.

We note the aberrant behavior of one low-uranium zircon (with ~128 ppm U). This grain shows a reversal to a smaller wavenumber after the second annealing at 1400 °C. After annealing at 1400 °C, this grain and two other low-uranium grains show values at or below the analytic boundaries of our measurements for synthetic uranium-free zircon grains. One effect might be that low-uranium zircon grains have a slower annealing rate because they are already close to the structure of undamaged zircon grains, and it might be more difficult to anneal such small damage. Another effect might be that in low-U zircon grains the compositional effect dominates and it is responsible for causing a shift in the Raman wavenumbers.

Radiation damage tends to accumulate more in high-uranium zircon grains due to abundant decay, and thus the annealing range revealed by the Raman measurements is naturally wider than in low-uranium zircon grains. This expectation is confirmed by our measurements. The wavenumber range for synthetic zircon grains with no uranium and no radiation damage (or natural zircon grains annealed sufficiently to remove all damage) is here referred to as "undamaged zircon" and the zircon grains corresponding to this frequency range as "end-member crystalline zircon."

For individual zircon grains that show distinct zoning, Raman spectroscopy reveals that the bright, more optically absorptive areas in the generally clear zircon grains show an increased intensity of the v_1 [SiO$_4$] symmetric stretching relative to the v_3 [SiO$_4$] antisymmetric stretching. The ratio of v_3/v_1 [SiO$_4$] Raman intensities decreases toward the bright areas, while the opposite effect occurs in the dark areas. The uranium concentrations determined by neutron irradiation, show that the bright areas
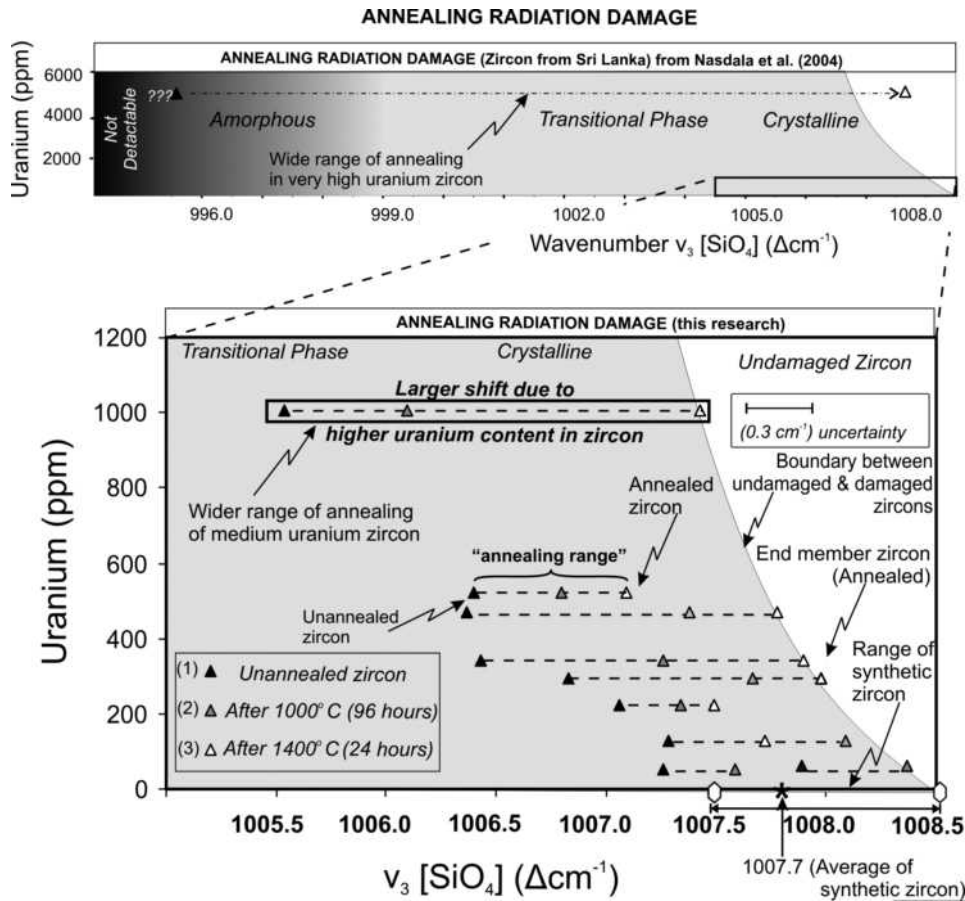
ANNEALING RADIATION DAMAGE

FIGURE 2. Raman measurements made on the same grains before annealing, and then after annealing at 1000 °C (96 h) and 1400 °C (24 h). The experiments indicate that high-uranium zircon grains show a larger shift to higher wavenumbers compared to low-uranium zircon. The difference of the minimum Raman wavenumber (higher radiation damage) and the maximum Raman wavenumber (annealed zircon grains with no radiation damage) of similar-uranium-zircon grains can be defined as the annealing range (*Diff* ΔR_U) of the radiation damage of zircon grains with similar uranium content and similar thermal history. During progressive annealing, the Raman spectra of all grains move toward the region of the uranium-free synthetic zircon grains that have no radiation damage (the undamaged end-member zircon).

have lower uranium concentration (~50–150 ppm), while areas of higher uranium concentration correspond to the darker areas (~300–400 ppm) in those zoned zircon grains. Raman measurements made on the same grains before and after annealing indicate that, after annealing, high-uranium grains (or zones if present) have dramatically increased Raman wavenumber values compared to low-uranium zircon grains (or zones).

Uranium and hafnium content

Halfnium in zircon affects the Raman wavenumber. Increasing hafnium concentration in our hafnium-doped synthetic zircon results in the position of (v_3, v_1) bands to higher vibrational frequencies and higher FWHM values (Marsellos 2008), which is consistent with the observations of Hoskin and Rodgers (1996). Hafnium is a common element in zircon that mostly ranges from 1–5 wt%. The Raman frequency (v_3) of hafnon is located at 1018 Δcm^{-1}, and so increasing the hafnium content of zircon results in a Raman wavenumber shift toward a higher frequency, while uranium content of zircon results in an opposite shift (lower frequency). However, the broadening of the FWHM is insignificant with increasing hafnium (Marsellos 2008), while the FWHM

broadens dramatically by increasing uranium concentration in zircon (discussed below).

Recall that grains with increasing radiation damage are identified by a Raman wavenumber shift to lower values. Raman measurements on zircon grains analyzed shows that radiation damage dominates this compositional effect in medium or higher uranium zircons. By contrast, in low-uranium zircons with short effective accumulation times, radiation damage is insignificant and compositional effects are more prominent. Finally, we note here that in low-uranium zircon grains with long effective accumulation times, radiation damage does become significant and the compositional effects may not be the prime factor for Raman wavenumber shifting.

The replacement of zirconium by hafnium shifts the frequency of v_3 [SiO$_4$] to higher wavenumbers but the accompanying change in the frequency of v_1 is insignificant. In contrast, increased uranium in the zircon tends to shift both v_1 and v_3 [SiO$_4$] frequencies to lower number and wider FWHM. The 57 hafnium- and uranium-free synthetic zircon grains with no radiation damage have an average v_3 [SiO$_4$] frequency of 1007.7 ± 0.3 Δcm^{-1} (Table 1), which is significantly lower than

the average frequency of the 40 synthetic hafnium-doped zircon grains. The synthetic zircon grains show an increase in FWHM (ν_3) (Marsellos 2008) with increasing hafnium concentration. Similar trends can be observed for the ν_1 [SiO$_4$] frequency, as well as for the FWHM of the ν_1 [SiO$_4$] frequency.

The Raman wavenumber from 67 zircon grains from the literature (Geisler et al. 2003; Nasdala et al. 2004, 2005) and the 435 zircon grains measured in this study covering a range from low to very high uranium concentration, show that there is a very good correlation for the position of the ν_3 [SiO$_4$] band (Fig. 3a), and for the FWHM of the ν_3 band (Fig. 3d). This result

shows that an estimate of the uranium content of zircon can be obtained from the FWHM or the frequency of the ν_3 [SiO$_4$] band. The ν_1 [SiO$_4$] Raman frequency shows also a good correlation to uranium content (Marsellos 2008).

IMPLICATIONS

Our experiments show that annealing at high temperatures restores radiation-damaged zircon to undamaged, end-member crystalline zircon. Raman measurements on the same grains before and after annealing indicate that after annealing at 1000 °C (for 96 h), high-uranium grains show a greater shift to higher

TABLE 1. Raman wavenumber frequencies of ν_1 and ν_3 [SiO$_4$] bands and their FWHM for the uranium-free synthetic zircons, with and without hafnium content

Synthetic zircon grains†	Hf (%wt)	U (%wt)	Freq. of ν_3 [SiO$_4$] (Δcm^{-1})	St. dev.* of ν_3 [SiO$_4$]	FWHM‡ of ν_3 [SiO$_4$] (cm^{-1})	St. dev.* of ν_3 FWHM	Freq. of ν_1 [SiO$_4$] (Δcm^{-1})	St. dev.* of ν_1 [SiO$_4$]	FWHM‡ of ν_1 [SiO$_4$] (cm^{-1})	St. dev.* of ν_1 FWHM
57	0	0	1007.7	0.19	2.5	0.27	974.2	0.16	2.2	0.12
5	0.8	0	1007.7	0.15	2.6	0.08	974.2	0.16	2.1	0.18
5	1.6	0	1007.8	0.40	2.6	0.13	974.2	0.26	2.1	0.06
15	3.2	0	1008.0	0.24	2.7	0.07	974.2	0.16	2.2	0.16
15	>3.2	0	1008.2	0.26	2.9	0.14	974.5	0.26	2.3	0.19

* St. dev. stands for standard deviation.
† Synthetic zircons have no radiation damage.
‡ FWHM values have been corrected according to Tanabe and Hiraishi (1980).
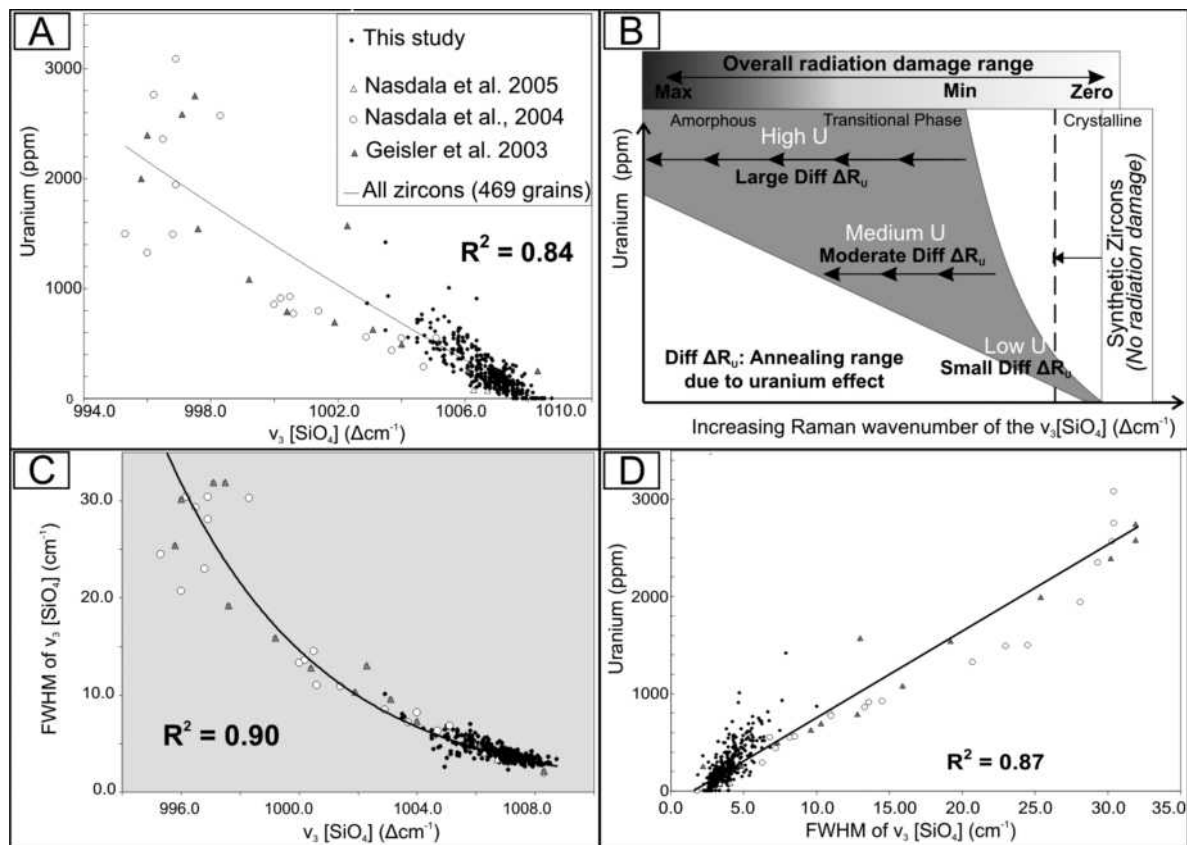

FIGURE 3. (**a**) Correlation between uranium content in zircon and the Raman wavenumber of the ν_3 [SiO$_4$] band frequency. (**b**) *Diff ΔR_U*: Annealing range of radiation damage in zircon grains from a quartzite on Peloponnese. The zircon grains have Paleozoic crystallization ages and they were affected by a Miocene thermal event: all were then annealed in the laboratory. The figure shows how uranium concentration affects the annealing range of the radiation damage in zircon with similar thermal history. The Raman wavenumber decreases with uranium concentration, reflecting the degree of saturation of the zircon by accumulated radiation damage (the proportion of the distorted to undistorted crystallinity in zircon). (**c**) Correlation between the full-width half maximum (FWHM) of the ν_3 [SiO$_4$] and the frequency ν_3 [SiO$_4$] of individual natural zircons. (**d**) Correlation between the FWHM of the ν_3 [SiO$_4$] plotted and the uranium content of individual natural zircon grains.

Raman wavenumbers compared to low-uranium zircon grains (Fig. 2). Further annealing at higher temperatures (1400 °C for 24 h) also shows that the previously annealed high-uranium grains show a larger shift to higher wavenumbers than the low-uranium zircon grains. In both cases, this change is toward the wavenumber range of undamaged end-member zircon (Fig. 2).

A key finding of this research is that zircon grains with a low to medium amount of uranium accumulate measureable radiation damage in proportion to the U-content. This finding is not surprising given what we know about the relationship between uranium and the damage that it causes by α-decay. High-uranium zircon will accumulate more radiation damage than low-uranium zircon in a given effective accumulation time. Therefore, the high-uranium zircon shows a wider wavenumber change after full annealing. This finding stands to reason because more uranium translates to a greater number of decay events. Raman spectroscopy measures the total radiation damage within a limited area/volume excited by the laser. An analytical problem arises when radiation damage is low in zircon grains of low-uranium content with short effective accumulation times. In these cases, the compositional effects—of uranium substitution in the crystal lattice—are most important in defining the Raman wavenumber of a particular grain. In zircon grains with low-uranium content

but long effective accumulation times, however, the radiation damage is significant and thus compositional effects may not be the prime factor of shifts in the Raman wavenumber.

The measured Raman parameters in our sample suite are correlated well with the uranium content of these zircon grains (Figs. 3a and 3d). Zircon grains of similar uranium content provide similar Raman spectral wavenumbers. The difference of the minimum Raman wavenumber (higher radiation damage) and the maximum Raman wavenumber (annealed zircon grains with no radiation damage) of similar uranium zircon grains (Fig. 3a) can be defined as the annealing range ($Diff\,\Delta R_U$) of the radiation damage of zircon grains with similar uranium content and similar thermal history (Fig. 3b). In grains with a narrow range in uranium, we find that radiation damage is the main component that contributes to the Raman wavenumber shift in this range of $Diff\,\Delta R_U$.

One key to understanding radiation damage may involve the different scales of development from the local intense radiation damage near a U or Th atom (atom-proximal) compared to the radiation damage density in the Raman measured volume and the entire zircon grain (Fig. 4). Overall radiation damage in a grain can be envisioned as "radiation damage density" in the zircon. In two zircon grains of similar crystallization age and thermal
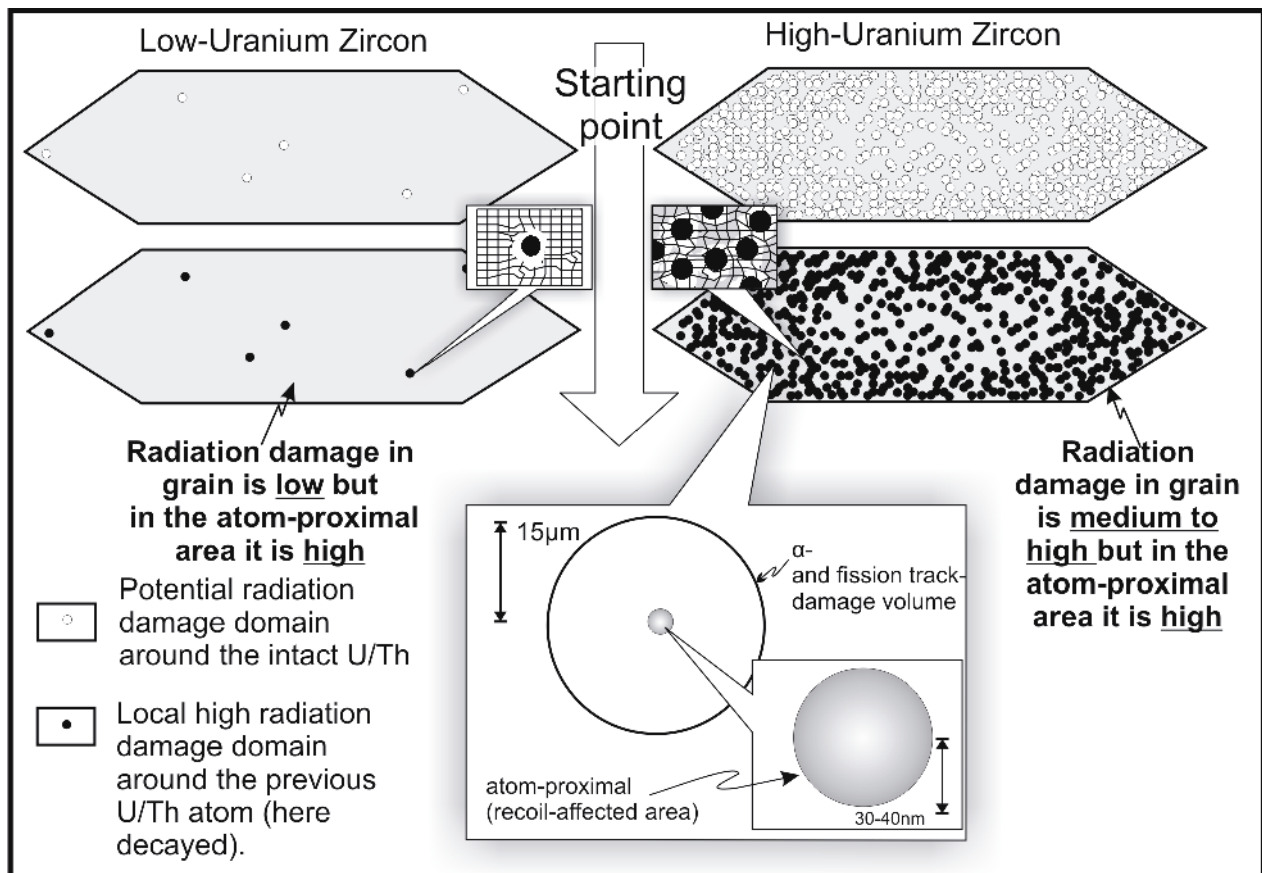

FIGURE 4. Radiation damage over the same accumulation time in low- and high-U,Th zircon. The radiation damage in the recoil-affected area around the daughter atom as well as the entire crystallinity of the zircon depends on the uranium/thorium in the grain. Low U,Th results in a small number of alpha, recoil, and fission events in the zircon host, and a low volume of overall radiation damage. In contrast, natural high-uranium zircon results in a much denser distribution of radiation damage compared to low-uranium zircon [radius of α-, fission track-damage, and recoil-affected volume from Weber (1993)].

history, the typical radiation damage density of a low-U,Th zircon is small compared to a grain with high U,Th concentration (Fig. 4). Another way to think of this is that a low-U,Th grain has a smaller number of decay events per unit volume compared to a high-U,Th grain over the same elapsed time. As such, low-U,Th zircons must be less affected by radiation over the same time interval, and in a low-uranium zircon, radiation damage varies from locally very high (Fig. 4) near a uranium domain (atom-proximal) to very low away from decayed U,Th sites [e.g., cf. Figs. 5b and 5c in Ewing et al. (2003)]. The radiation damage that Raman spectroscopy is able to detect is the radiation damage from a relatively large volume of the zircon (partly because it is a function of irradiation volume of the laser), and therefore in low-uranium zircon grains, the radiation damage is low regardless of the strong damage around the local uranium atom sites.

Over time, the radiation damage in a uranium-bearing zircon must increase provided the ambient temperature is below the threshold for thermal annealing. This temperature range is not well studied in geological samples [for a discussion of this in the context of the ZFT system, see Garver and Kamp (2002) and Garver et al. (2005)]. In very high-uranium zircon grains, the radiation damage implied by v_3 [SiO$_4$] frequency is revealed in the very broad range of Raman wavenumbers. This increasing annealing range corresponding to an increase in uranium content implies that there is more damage in higher uranium zircon grains (Figs. 3a and 3b). The radiation damage range is constrained by Raman wavenumber frequencies of amorphous zircon grains (the smallest wavenumber of v_3 or/and v_1 [SiO$_4$] frequencies that can still reveal a [SiO$_4$] signal from the zircon) and end-member undamaged zircon. An extremely long accumulation time would be required for a low-uranium zircon to approach the same amount of radiation damage as a high-uranium zircon, for both to show equal radiation damage as measured by Raman spectroscopy. Therefore, time is the key distinguishing variable for the amount of radiation damage in zircon grains having the same uranium concentration. As such, radiation damage that can be revealed by Raman measurements may provide a new way to measure cooling ages (Fig. 5) in suites of zircon grains with a wide spectrum of radiation damage.

In a suite of nearly homogeneous zircon grains from volcanic rocks (i.e., quick-cooled and with generally a narrow range of composition), radiation damage from grain to grain is relatively uniform. In this case, we note that all zircon grains have a very good correlation between Raman wavenumber and radiation damage. To examine this relationship, we looked at zircon from the Oligocene Fish Canyon Tuff, a widely used standard in zircon fission track dating (see Garver 2003). However, the situation we present in this paper is one where detrital zircon grains have fully annealed fission tracks but very different degrees of radiation damage because grains had dramatically different histories prior to deposition. Therefore, although the grains have a similar post-depositional history, the annealing of α-damage was highly variable. Pidgeon et al. (1998) suggested the potential for using Raman spectroscopy for determining structural damage ages in zircon. They suggested that for spots analyzed with Sensitive High-Resolution Ion MicroProbe (SHRIMP) that discordance should be compared with degree of radiation damage, which should provide information on the conditions and timing of an-

nealing of damage (Pidgeon et al. 1998). Here, we discuss a possible relationship between Raman wavenumber measurements of v_3 [SiO$_4$] and uranium content of individual zircon grains that may shed light on determining the radiation damage age of zircon and how this is useful and relevant for FT dating.

Regardless of the uranium content and crystallization age, the Raman wavenumber and FWHM variation appears to be a useful measure of radiation damage in zircon. It is also known that radiation damage dramatically affects the annealing characteristics of fission tracks (Kasuya and Naeser 1988). Finally, we note that studies of samples from orogenic belts show that heated detrital zircon grains show a wide variation in ages from a single sample that can be ascribed to annealing kinetics that vary from grain to grain. This grain-to-grain difference in annealing appears to be affected by total internal damage in a zircon (see Brandon et al. 1998; Garver et al. 2005), but there remains some question if there is a compositional effect. Nonetheless, there are a few basic observations that are important to understanding this system. Zircon grains with low damage are more resistant to annealing and have a higher effective closure temperature compared to those with high damage (see Rahn et al. 2004; Garver et al. 2005). One hope is that the range of v_3 and FWHM values may be used as a proxy for radiation damage and therefore in discriminating high- from low-retentive zircon grains. So, we are interested in using Raman measurements to measure radiation damage, but to do this we must first remove the effect of uranium on the Raman signal.

A mathematical approach to quantifying radiation damage is attempted using Raman measurements. To eliminate the contribution of uranium to get a sense of radiation damage alone, we begin with the logarithmic value of uranium content in ppm (log U). Squaring the difference between the Raman wavenumber v_3 and the maximum possible value in undamaged zircon [$d^2 = (v_3 - 1008.5)^2$] allows for a separation of high- to low-retentive zircon grains. This approach stems from the fact that values above 1007.5 Δcm^{-1} approach the end-member non-radiation-damaged zircon grains.
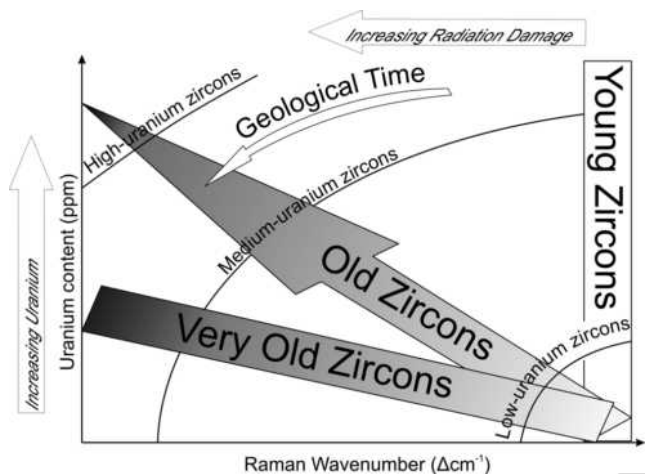

FIGURE 5. Low-uranium zircon needs a long time to accumulate the same amount of damage compared to high-uranium zircon. Time is what distinguishes zircon grains of the same uranium concentration with different radiation damage.

Each grain measured by Raman spectroscopy has several properties, including the position and FWHM of ν_3, uranium content, and FT age of the most recent thermal event, which may be primary factors in determining radiation damage. Because radiation damage is described primarily by FWHM and ν_3 position and because the effect of uranium needs a first approximation at the discrimination of high-retentive zircon grains (of minimum radiation damage) from low-retentive zircon grains (of maximum radiation damage), then a proxy for radiation damage could be defined by the following formula

$$Z_{RDD} = \log U \cdot FWHM \cdot (1008.5 - \nu_3)^2. \tag{1}$$

This approach is used on annealed and partly annealed grains analyzed in this study (Fig. 6). The relationship between zircon fission-track grain age (ZFTGA) and radiation damage discrimination (Z_{RDD}) shows that the grains in our test case fall in three relatively distinct regions (fields A, B, and C). Field A represents fully annealed zircons that have less radiation damage and young fission tracks and no old fission tracks since crystallization. Field B represents the zircons that have more radiation damage and no old fission tracks and therefore this field is fully reset and likely low-retentive zircon. Intuitively it is not clear why any zircon grain would fall into field C considering T_{max} these rocks experienced (ca. 350 °C, see discussion on Theye et al. 1992). Field C represents zircon grains that have substantial radiation damage and many old unannealed or partially annealed fission tracks. One possibility for this field (field C) is that these grains had extreme damage and very high track densities prior to annealing and recovery was not possible for α-damage nor fission damage given the maximum temperatures the rock experienced. Our preliminary U/Pb ages on these grains show

that they have Precambrian crystallization ages (Marsellos and Garver, unpublished manuscript). Another possibility is that these grains have some other factor, such as crystal chemistry, that hinders annealing.

Of interest in this data set are those grains that have had fission tracks annealed, and these appear to fall into two groups: one with high radiation damage and young FT ages (field B), and one with low radiation damage and young FT ages (field A). An important question is whether these data change our approach to determining a ZFT age for such a sample. Traditional ZFT analysis of this sample results in an over-dispersed grain-age distribution, which means that despite heating and annealing of almost all zircon grains, the age distribution falls outside a normal Gaussian distribution. We know that the over-dispersion is quite common in heated detrital zircon grains and the wide range in grain ages is typically interpreted to reflect heterogeneity of track annealing due to radiation damage as discussed above. Nonetheless, a standard approach is to apply a binomial peak-fitting technique to isolate the young population of grain ages (see Brandon 1996), and in this case the approach yields a young ZFT age of 9.2 ± 1.5 Ma. However, we are curious if the radiation damage discrimination can isolate a retentive population and a less retentive population of reset zircon grains. If so, these young ages may have geological significance and they may allow refinement of the young reset age.

We suspect that the high-damage reset (HDR) grains (field B) define the single best estimate of final closure of the ZFT system for this sample. The HDR grains form a single component age of 7.0 ± 1.4 Ma, compared to the young population of 9.2 ± 1.5 Ma derived from traditional binomial peak fitting of all grains. It is interesting to note that these grains tend to have the lowest concentrations of thorium as revealed in our U/Pb analyses of
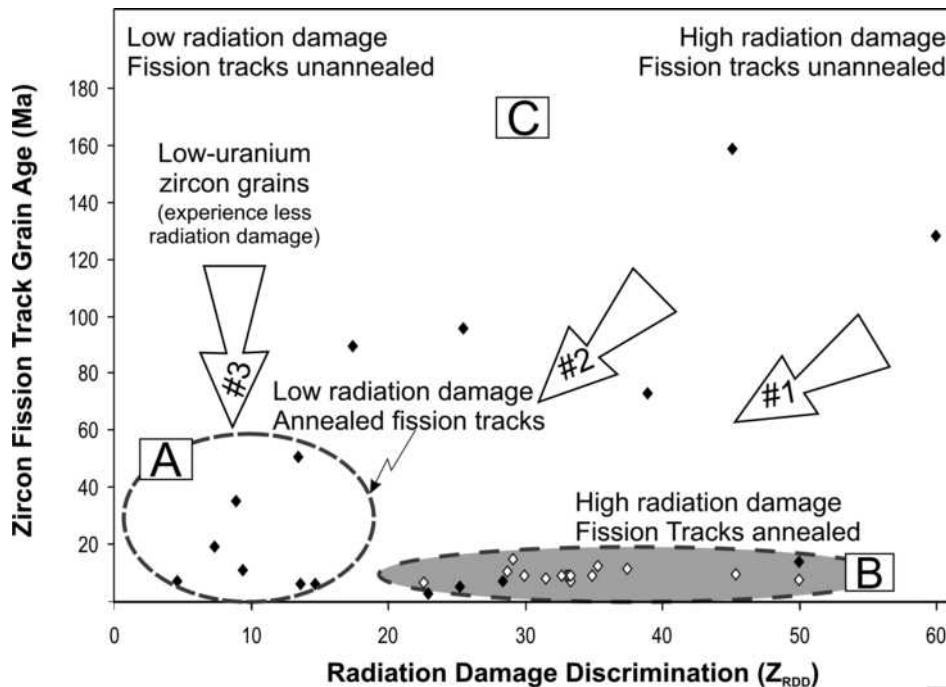

FIGURE 6. Graph shows three different annealing paths from (arrow 1) low-, (arrow 2) medium-, and (arrow 3) high-radiation damaged zircons. White diamonds are zircon grains from a fully reset sample and the black diamonds are zircon grains from a partially to fully reset sample.

single grains. Grains that fall in field A are low-damage reset (LDR) grains that clearly are over-dispersed, meaning they fall outside a normal Gaussian distribution for a single population. In this case, they are more difficult to interpret with confidence. Of all the grains in this data set, those in field A have the lowest uranium concentration. We suspect that these LDR grains are a mixture of high- and low-retentive zircon grains and applying traditional binomial peak-fitting statistics on this group yields two component populations: one (P1) at 7.5 ± 2.6 Ma and one (P2) at 36.1 ± 7.2 Ma. Therefore, a component age based on these LDR grains (field A) has less geological significance, because it contains some zircons that are not fully reset or partly reset. Population P2 from the LDR grains is likely meaningless as it is comprised mainly of grains that are partly reset. Finally we note that un-reset grains with variable but generally high radiation damage (field C) have ZFT ages (ca. 90–160 Ma) that are, essentially, meaningless (single population at 116 ± 11 Ma). We cannot rule out partial annealing of these grains, and therefore at best they only provide a minimum age of cooling of the source terrain that supplied sediments to the basin (i.e., here, mid-Cretaceous or older). As we suggest above, it is possible that these grains had too much damage to anneal during the relatively brief residence of these rocks at depths with elevated temperatures. In fact, our preliminary U/Pb analysis shows that this population (field C) is comprised exclusively of Precambrian grains.

Therefore, we are encouraged that the separation of low-retentive zircons using the Zircon Radiation Damage Discrimination factor (Z_{RDD}) provides a new tool that allows refinement of the cooling ages of overdispersed samples that show characteristics of heterogeneous annealing. Z_{RDD} is the first non-statistical approach (based on mineralogical properties) that may be used to isolate non-retentive FT-dated zircon grains. The Z_{RDD} cooling age of 7.0 ± 1.4 Ma provides new insight into the tectonothermal evolution of the phyllite-quartzite-rocks (PQ unit) from the Hellenic forearc (Seidel et al. 1982; Theye et al. 1991, 1992; Gerolymatos 1994). While this result is intriguing, we note that the data are limited, and this problem warrants further study.

CONCLUDING REMARKS

An important finding of our work is that the Raman wavenumber in zircon is a function of uranium concentration, which is consistent with previous studies (Wopenka et al. 1996; Geisler et al. 2005). Uranium content and other compositional effects, crystallization age, and the radiation damage contribute to the Raman wavenumber shift and FWHM values. After time, radiation damage becomes the main component, because it affects the crystal structure that Raman spectroscopy measures.

Our findings resulted from our analytical approach that paired fission-track dating and Raman analysis of individual FT-dated grains. Because our ultimate goal is to understand radiation damage and how it affects annealing and track retention in zircon, we find that we are in need of synthetic uranium-doped zircon with no radiation damage. These synthetic zircons would allow a better understanding of the relationship between uranium and Raman wavenumber.

Our annealing experiments show that radiation damage is removed progressively and that annealed grains have better internal ordering. It is clear that α-particle damage affects the

thermal stability of fission tracks, therefore it is a key property that needs to be understood in studies of fission-track retention in zircon (i.e., Kasuya and Naeser 1988; Carter 1990; Rahn et al. 2004; Tagami 2005). But what remains to be done are experiments that relate the annealing of fission tracks to radiation damage as measured by Raman spectroscopy.

REFERENCES CITED

Ahrens, L.H. (1965) Some observations on the uranium and thorium distribution in accessory zircons from granitic rocks. Geochimica et Cosmochimica Acta, 29, 711–716.
Ahrens L.H. and Erlank A.J. (1969) Hafnium. In K.H. Wedepohl, Ed., Handbook of Geochemistry, vol. 2, part 5, sections B–O. Springer-Verlag, Berlin.
Ahrens, L.H., Cherry, R.D., and Erlank, A.J. (1967) Observations on the Th-U relationship in zircons from granitic rocks and from kimberlites. Geochimica et Cosmochimica Acta, 31, 2379–2387.
Balan, E., Neuville, D.R., Trocellier, P., Fritsch, E., Muller, J.-P., and Calas, G. (2001) Metamictization and chemical durability of detrital zircon. American Mineralogist, 86, 1025–1033.
Bernet, M. and Garver, J.I. (2005) Fission-track analysis of Detrital zircon. In P.W. Reiners and T.A. Ehlers, Eds., Low-temperature Thermochronology: Techniques, interpretations, and applications, 58, p. 205–237. Reviews in Mineralogy and Geochemistry, Mineralogical Society of America, Chantilly, Virginia.
Brandon, M.T. (1996) Probability density plot for fission-track grain-age samples. Radiation Measurements, 26, 663–676.
Brandon, M.T., Roden-Tice, M.K., and Garver, J.I. (1998) Late Cenozoic exhumation of the Cascadia accretionary wedge in the Olympic Mountains, northwest Washington State. Bulletin of the Geological Society of America, 110, 985–1009.
Carter, A. (1990) The thermal history and annealing effects in zircons from the Ordovician of North Wales. Nuclear Tracks and Radiation Measurements, 17, 309–313.
Chakoumakos, B.C., Murakami, T., Lumpkin, G.R., and Ewing, R.C. (1987) Alpha-decay–induced fracturing in zircon: the transition from the crystalline to the metamict state. Science, 236, 1556–1559.
Ellsworth, S., Navrotsky, A., and Ewing, R.C. (1994) Energetics of radiation damage in natural zircon ($ZrSiO_4$). Physics and Chemistry of Minerals, 21, 140–149.
Ewing, R.C. (1994) The metamict state: 1993—The centennial. Nuclear Instruments and Methods in Physics Research B, 91, 22–29.
Ewing, R.C., Meldrum, A., Wang, L., Weber W.J., and Corrales, L.R. (2003) Radiation effects in zircon. In J.M. Hanchar and P.W.O. Hoskin. Eds., Zircon, 53, p. 378–420. Reviews in Mineralogy and Geochemisty, Mineralogical Society of America, Chantilly, Virginia.
Farnan, I. and Salje, E.K.H. (2001) The degree and nature of radiation damage in zircon observed by ^{29}Si nuclear magnetic resonance. Journal of Applied Physics, 89, 2084–2090.
Fleischer, R.L. (2003) Etching of recoil tracks in solids. Geochimica et Cosmochimica Acta, 67, 4769–4774.
Garver, J.I. (2003) Etching age standards for fission track analysis. Radiation Measurements, 37, 47–54.
——— (2008) Fission-track dating. In V. Gornitz, Ed., Encyclopedia of Paleoclimatology and Ancient Environments, p. 247–249. Encyclopedia of Earth Science Series, Springer, Berlin.
Garver, J.I. and Kamp, P.J.J. (2002) Integration of zircon color and zircon fission-track zonation patterns in orogenic belts: Application to the Southern Alps, New Zealand. Tectonophysics, 349, 203–219.
Garver, J.I., Reiners, P.R., Walker, L.J., Ramage, J.M., and Perry, S.E. (2005) Implications for timing of Andean uplift based on thermal resetting of radiation-damaged zircon in the Cordillera Huayhuash, northern Perú. Journal of Geology, 113, 117–138.
Geisler, T. (2002) Isothermal annealing of partially metamict zircon: evidence

for a three-stage recovery process. Physics and Chemistry of Minerals, 29, 420–429.

Geisler, T., Pidgeon, R.T., van Bronswijk, W., and Pleysier, R. (2001) Kinetics of thermal recovery and recrystallization of partially metamict zircon: A Raman spectroscopic study. European Journal of Mineralogy, 13, 1163–1176.

Geisler, T., Pidgeon, R.T., van Bronswijk, W., and Kurtz, R. (2002) Transport of uranium, thorium, and lead in metamict zircon under low-temperature hydrothermal conditions. Chemical Geology, 191, 141–154.

Geisler, T., Pidgeon, R.T., Kurtz, R., van Bronswijk, W., and Schleicher, H. (2003a) Experimental hydrothermal alteration of partially metamict zircon. American Mineralogist, 86, 1496–1518.

Geisler, T., Trachenko, K., Rios, S., Dove, T.M., and Salje, E.K.H. (2003b) Impact of self-irradiation damage on the aqueous durability of zircon ($ZrSiO_4$): Implications for its suitability as a nuclear waste form. Journal of Physics, Condensed Matter, 15, 597–605.

Geisler, T., Burakov, B.E., Zirlin, V., Nikolaeva, L., and Poml, P. (2005) A Raman spectroscopic study of high-uranium zircon from the Chernobyl "lava." European Journal of Mineralogy, 17, 883–894.

Gerolymatos, I.K. (1994) Metamorphose und Tectonik der Phyllit-Quartzit-Serie und der Tyros-Schichten auf dem Peloponnese und Kythira. Berliner Geowissenschaftliche Abhandlungen. Reihe A: Geologie und Palaontologie, 164, 1–101.

Hogdahl, K., Gromet, L.P., and Broman, C. (2001) Low P-T Caledonian resetting of U-rich Paleoproterozoic zircons, central Sweden. American Mineralogist, 86, 546–562.

Holland, H.D. and Gottfried, D. (1955) The effect of nuclear radiation on the structure of zircon. Acta Crystallographica, 8, 291–300.

Hoskin, P.W.O. and Rodgers, K.A. (1996) Raman spectral shift in the isomorphous series $(Zr_{1-x}Hf_x)SiO_4$. European Journal of Solid State Inorganic Chemistry, 33, 1111–1121.

Kasuya, M. and Naeser, C.W. (1988) The effect of α-damage on fission-track annealing in zircon. Nuclear Tracks and Radiation Measurements, 14, 477–480.

Marsellos, A.E. (2008) Extension and exhumation of the Hellenic forearc; and radiation damage in zircon, p. 754. Doctoral Dissertation, University at Albany, New York.

Marsellos, A.E., Kidd, W.S.F., and Garver, J.I. (2010) Extension and exhumation of the HP/LT rocks in the Hellenic forearc ridge. American Journal of Science, 310, 1–36.

Nasdala, L., Irmer, G., and Wolf, D. (1995) The degree of metamictization in zircon: A Raman spectroscopic study. European Journal of Mineralogy, 7, 471–478.

Nasdala, L., Pidgeon, R.T., Wolf, D., and Irmer, G. (1998) Metamictization and U-Pb isotopic discordance in single zircons: A combined Raman microprobe and SHRIMP ion probe study. Mineralogy and Petrology, 62, 1–27.

Nasdala, L., Wenzel, M., Vavra, G., Irmer, G., Wenzel, T., and Kober, B. (2001) Metamictisation of natural zircon: accumulation vs. thermal annealing of radioactivity-induced damage. Contributions to Mineralogy and Petrology, 141, 125–144.

Nasdala, L., Zhang, M., Kempe, U., Panczer, G., Gaft, M., Andrut, M., and Plötze, M. (2003) Spectroscopic methods applied to zircon. In J.M. Hanchar and P.W.O. Hoskin, Eds., Zircon, 53, p. 427–467. Reviews in Mineralogy and Geochemistry, Mineralogical Society of America, Chantilly, Virginia.

Nasdala, L., Reiners, P.W., Garver, J.I., Kennedy, A.K., Stern, R.A., Balan, E., and Wirth, R. (2004) Incomplete retention of radiation damage in zircon from Sri Lanka. American Mineralogist, 89, 219–231.

Nasdala, L., Hanchar, J.M., Kronz, A., and Whitehouse, M.J. (2005) Long-term stability of alpha particle damage in natural zircon. Chemical Geology, 220, 83–103.

Palenik, C.S., Nasdala, L., and Ewing, R.C. (2003) Radiation damage in zircon. American Mineralogist, 88, 770–781.

Pidgeon, R.T., Nasdala, L., and Todt, W. (1998) Determination of radiation damage ages on parts of zircon grains by Raman microprobe: Implications for annealing

history and U-Pb stability. Mineralogical Magazine, 62A, 1174–1175.

Rahn, M.K., Brandon, M.T., Batt, G.E., and Garver, J.I. (2004) A zero-damage model for fission-track annealing in zircon. American Mineralogist, 89, 473–484.

Reiners, P.W. (2005) Zircon (U-Th)/He thermochronometry, In P.W. Reiners and T.A. Ehlers, Eds., Low-temperature Thermochronology: Techniques, interpretations, and applications, 58, p. 151–176. Reviews in Mineralogy and Geochemistry, Mineralogical Society of America, Chantilly, Virginia.

Seidel, E., Kreuzer, H., and Harre, W. (1982) A Late Oligocene/Early Miocene High Pressure Belt in the External Hellenides. Geologisches Jahrbuch, E23, 165–206.

Shannon, R.D. (1976) Revised effective ionic radii and systematic studies of interatomic distances in Halides and Chalcogenides. Acta Crystallographica, A32, 751.

Speer, J.A. (1980) Zircon. In P.H. Ribbe, Ed., Orthosilicates, 2nd edition, 5, p. 67–112. Reviews in Mineralogy, Mineralogical Society of America, Chantilly, Virginia.

Speer, J.A. and Cooper, B.N. (1982) Crystal structure of synthetic hafnon, $HfSiO_4$, comparison with zircon and the actinide orthosilicates. American Mineralogist, 67, 804–808.

Tabaksblat, R., Meier, R.J., and Kip, B.J. (1992) Confocal Raman microspectroscopy: Theory and application to thin polymer samples. Applied Spectroscopy, 46, 60–68.

Tagami, T. (2005) Zircon fission-track thermochronology and applications to fault studies. In P.W. Reiners and T.A. Ehlers, Eds., Low-temperature Thermochronology: Techniques, interpretations, and applications, 58, p. 95–122. Reviews in Mineralogy and Geochemistry, Mineralogical Society of America. Geochemical Society, Chantilly, Virginia.

Theye, T. and Seidel, E. (1991) Petrology of low-grade high-pressure metapelites from the external Hellenides (Crete, Peloponnese). A case study with attention to sodic minerals. European Journal of Mineralogy, 3, 343–366.

Theye, T., Seidel, E., and Vidal, O. (1992) Carpholite, sudoite, and chloritoid in low-grade high-pressure metapelites from Crete and the Peloponnese, Greece. European Journal of Mineralogy, 4, 487–507.

Wagner, G. and Van Den Haute, P. (1992) Fission Track Dating, 283 p. Kluwer Academic Publishers, Dordrecht.

Weber, W.J. (1993) Alpha-decay-induced amorphization in complex silicate structures. Journal of American Ceramic Society, 76, 1729–1738.

Weber, W.J., Ewing, R.C., and Wang, L.-M. (1994) The radiation-induced crystalline-to-amorphous transition in zircon. Journal of Materials Research, 9, 688–698.

Woodhead, J.A., Rossman, G.R., and Silver, L.T. (1991) The metamictization of zircon: Radiation dose-dependent characteristics. American Mineralogist, 76, 74–82.

Wopenka, B., Jolliff, B.L., Zinner, E., and Kremser, D.T. (1996) Trace element zoning and incipient metamictization in a lunar zircon: Application of three microprobe techniques. American Mineralogist, 81, 902–912.

Zhang, M., Salje, E.K.H., Farnan, I., Graeme-Barber, A., Daniel, P., Ewing, R.C., Clark, A.M., Rios, S., and Leroux, H. (2000a) Metamictization of zircon: Raman spectroscopic study. Journal of Physics: Condensed Matter, 12, 1915–1925.

Zhang, M., Salje, E.K.H., Farnan, I., Capitani, G.C., Leroux, H., Clark, A.M., Schlüter, J., and Ewing, R.C. (2000b) Annealing of α-decay damage in zircon: A Raman spectroscopic study. Journal of Physics: Condensed Matter, 12, 3131–3148.